# Enhancement in Light Output of InGaN-Based Microhole Array Light-Emitting Diodes

T. H. Hsueh, J. K. Sheu, H. W. Huang, J. Y. Chu, C. C. Kao, H. C. Kuo*, Member, IEEE*, and S. C. Wang*, Senior Member, IEEE*

***Abstract*—InGaN-based microhole array light-emitting diodes (LEDs) with hole diameters ($d$) of 3–15 $\mu$m were fabricated using self-aligned etching. The effects of size on the device characteristics, including current density–voltage and light output–current density, were measured and compared with those of conventional broad-area (BA) LEDs fabricated from the same wafer. The electrical characteristics of the devices are similar to those of conventional BA LEDs. The light output from the microhole array LEDs increases with $d$ up to 7 $\mu$m. However, the light output declined as $d$ increased further, perhaps because of the combination of the enhancement in extraction efficiency caused by the large surface areas provided by the sidewalls and the decrease in area of light generation by holes in the microhole array LEDs. The ray tracing method was used with a two-dimensional model in TracePro software. The findings indicate that an optimal design can improve the light output efficiently of the microhole array LEDs.**

***Index Terms*—GaN, micro-light-emitting diode ($\mu$-LED), quantum well (QW).**

## I. INTRODUCTION

InGaN-based quantum-well (QW) light-emitting diodes (LEDs) are affecting the development of full-color displays, illumination, and exterior automotive lighting over a spectral range from near ultraviolet to green and amber. Devices are grown epitaxially on either sapphire or silicon carbide substrates and their structure contains a single InGaN–GaN QW active region sandwiched between two GaN layers. The absorption coefficient of GaN in the photon-energy range from 2.0 to 3.1 eV is approximately $3 \times 10^2$ cm$^{-1}$ [1], so some of the light from the active region is absorbed before it leaves out the devices. Furthermore, approximately $1/(4\,n^2)$ of the light from the active region radiates through the top and bottom of the devices because of guided modes in which light is totally reflected between the device surface and the air [2]. (The GaN refractive index $n$ is ~2.4.) Recently, III–nitride micro-LEDs ($\mu$-LEDs) have attracted great interest in the area of high-extraction efficiency optoelectronic devices. Many groups have reported high-performance GaN-based microdisk and microring LEDs [3]–[7]. These $\mu$-LEDs are generally accepted to have greater light output efficiencies than their broad-area (BA) conventional LED counterparts because the (re)absorption of light is reduced on the micrometer scale. Additionally, their greater extraction efficiency relative to the BA devices is attributable to the scattering of light from the etched sidewall surfaces and the great increase in the surface areas of the $\mu$-LEDs [3]–[5]. However, the decline in the area of light-generation of the $\mu$-LEDs may significantly affect their light output performance. This work reports on the design, fabrication, and characteristics of InGaN-based LEDs microhole array LEDs. The effects of the decline in the area of the active region on light output by microhole array LEDs were also investigated in detail.

## II. DEVICE FABRICATION

The examined samples were grown on $c$-plane sapphire substrates with a 30-nm-thick GaN nucleation layer by metal–organic chemical vapor deposition. The LED structure contains a 4-$\mu$m-thick Si-doped n-GaN; an active layer of five-period $\mathrm{In_{0.2}Ga_{0.8}N}$ (3 nm)/GaN (7 nm) QWs; a 50-nm-thick Mg-doped $\mathrm{Al_{0.15}Ga_{0.75}N}$ layer; and a 0.25-$\mu$m-thick Mg-doped p-GaN. Finally, samples topped with a contact layer of 50-pair Si-doped $\mathrm{n^+}$-$\mathrm{In_{0.23}Ga_{0.77}N}$–GaN short-period superlattices rather than high-resistivity p-GaN to reduce the p-contact resistance and improve the current spreading [8]. The wafer growth procedures are reported in detail elsewhere [9].

The processing of the InGaN-based microhole array LEDs began with electron-beam evaporated Ni (5 nm)/Au (8 nm) to form a high-transparency p-type Ohmic contact [10]. The holes and the rectangular mesa (360 $\times$ 250 $\mu$m) were fabricated simultaneously by photolithographic patterning, the wet etching of Ni–Au layers, and inductively coupled plasma (ICP) self-aligned dry etching (SAMCO ICP-RIE 101iPH). The dry etching was performed in a gas mixture of $\mathrm{Cl_2}$–Ar $= 10/25$ sccm with an ICP source power of 400 W, a bias power of 40 W, and a chamber pressure of 5 mTorr. The effect of pattern-dependent etching on the microhole array LEDs is not obvious under these etching conditions. The samples were then etched down to the n-GaN layer with an approximate depth of 1.2 $\mu$m. The diameters of the holes were 3, 7, 11, and 15 $\mu$m, as determined using a scanning electronic microscope measurement. Spacing between two holes was fixed at 25 $\mu$m. Notably, the procedures for fabricating the microhole array LEDs are identical to those for fabricating conventional BA LEDs. Thermal annealing was applied to the p-type contact alloy at 500 °C in air for 5 min. Finally,

---

Manuscript received December 16, 2004; revised February 2, 2005. This work was supported in part by the National Science Council of the Republic of China (R.O.C.) in Taiwan under Contract 93-2120-M-009-006.

T. H. Hsueh, H. W. Huang, J. Y. Chu, C. C. Kao, H. C. Kuo, and S. C. Wang are with the Department of Photonics, Institute of Electro-Optical Engineering, National Chiao Tung University, Hinchu 300, Taiwan, R.O.C. (e-mail: taohung.eo90g@nctu.edu.tw; stevenhuang@truelight.com.tw; rychu.eo92g@mctu.edu.tw; kdicky.eo91g@nctu.edu.tw; hckuo@faculty.nctu.edu.tw; scwang@mail.nctu.edu.tw).

J. K. Sheu is with the Institute of Electro-Optical Science and Engineering, National Cheng Kung University, Tainan 701, Taiwan, R.O.C. (e-mail: jksheu@mail.ncku.edu.tw).

Digital Object Identifier 10.1109/LPT.2005.846459

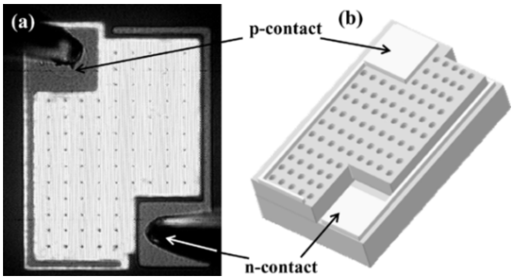

Fig. 1. (a) Optical microscope image of a 360 × 250 $\mu$m microhole array LED with $d = 7$ $\mu$m. (b) Schematic diagram of a representative microhole array LED fabricated by photolithography patterning and dry etching.

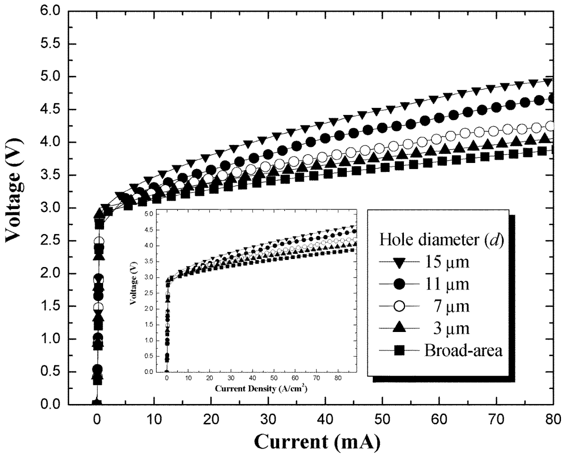

Fig. 2. Curves of $I$–$V$ of microhole array LEDs and a conventional BA LED fabricated from the same wafer. The insert is the current $J$–$V$ curves of the devices.

the trilayers of Ti–Pt–Au (50/20/200 nm) for p-type pad were deposited. Fig. 1(a) shows an optical microphotograph of the top of a microhole array LED chip and $d = 7$ $\mu$m. Fig. 1(b) schematically depicts a microhole array LED. The conventional BA LEDs with the same mesa size (360 × 250 $\mu$m) were also fabricated from the same wafer for comparison. The typical current–voltage ($I$–$V$) measurements were performed using a high current measure unit (KEITHLEY 238). The light output power was measured using a calibrated power meter with a large Si detector (detector area 10 × 10 mm$^2$) approximate 5 mm above the device, collecting the light emitted in the forward direction.

## III. RESULT AND DISCUSSION

Fig. 2 plots the $I$–$V$ characteristics of the microhole array LEDs with different values of $d$ and that of a conventional BA LED fabricated from the same wafer. The devices have unequal area of light generation, so the insert in Fig. 2 plots the current density–voltage [($J$–$V$) evaluated by taking the ratio of the actual driving currents to their active areas]. The forward bias voltage $V_F$ at a driving current of 20 mA increases with $d$ ($V_F = 3.38, 3.41, 3.57$, and 3.80 V for $d = 3, 7, 11$, and 15 $\mu$m) and slightly exceeds that of the conventional BA LED ($V_F = 3.28$ V). The $J$–$V$ characteristic is similar to the $I$–$V$ characteristic in Fig. 2. Additionally, the operating voltages of the microhole array LEDs marginally exceed those of the conventional BA LED, because of the reduction in the total active area [3], [4], [11] and the presence of a plasma-damage region parallel to the sidewalls within the holes [12]. The holes were fabricated by dry etching; plasma damage occurs on the sidewalls, increasing the surface recombination of the injected electrons and holes.

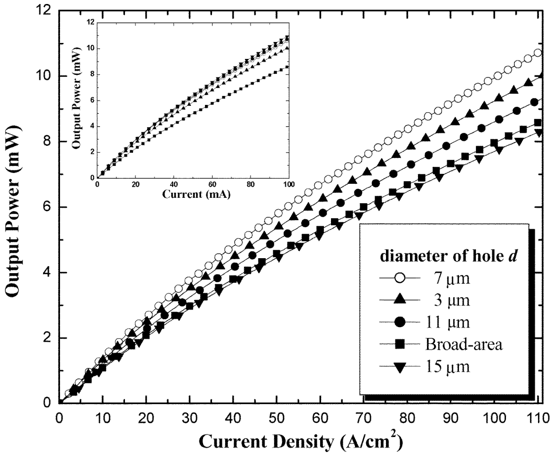

Fig. 3. Light output power of microhole array LEDs and a conventional BA LED as functions of injected current density. The insert shows the light output power–current ($L$–$I$) curves.

Fig. 3 plots the light output–current density ($L$–$J$) curves. The microhole array LED with $d = 7$ $\mu$m has a light output power of ~3.0 mW at 22.2 A/cm$^2$ (corresponding to a driving current of 20 mA for the conventional BA LED), which is 36% greater than ~2.2 mW for the conventional BA LED. Moreover, the light output power of the microhole array LEDs decreases as the $d$ increases above 11 $\mu$m and the light output power of the microhole array LED with $d = 15$ $\mu$m is less than that of the conventional BA LED. The insert in Fig. 3 plots the light output–current ($L$–$I$) curves. The light output power increases as $d$ increases, being distinct from the $L$–$J$ curves. Notably, the $L$–$I$ curves are similar as $d$ increases above 7 $\mu$m. The light output by an optoelectronic device is governed by the internal quantum efficiency and extraction efficiency. Internal quantum efficiency is a natural property of LEDs; the geometry of the device strongly influences the extraction efficiency. Fig. 4(a) and (b) presents the emission image and the intensity profile of a microhole array LED with $d = 7$ $\mu$m at an operating current of 1 mA, respectively. A bright luminescence ring is observed at the periphery of the hole, similar to that observed in micropillar LEDs [3]. Most of the light propagated in the plane is emitted through the surface of the sidewall, but scattering on the etched sidewall causes some of the light to be extracted from the top surface near the periphery, causing the ring of light to be observed in the emission images, and increasing the light output in the forward direction.

The propagation and reflection of light in the devices were examined by applying the ray tracing method associated with the two-dimensional model in TracePro [13], [14]. The parameters used in the simulation were: refractive index of GaN = 2.4, absorption coefficient = 100 cm$^{-1}$, refractive index of AlGaN = 2.2, and transmission of

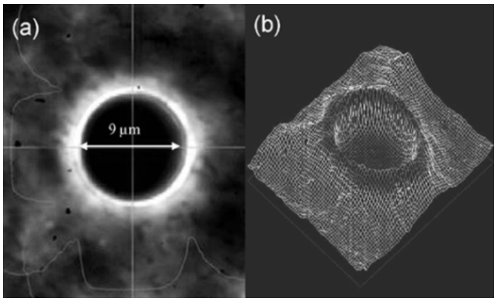

Fig. 4. Showing (a) microphotograph and (b) emission profile of a microhole array LED with $d = 7\ \mu$m at 1-mA driving current.

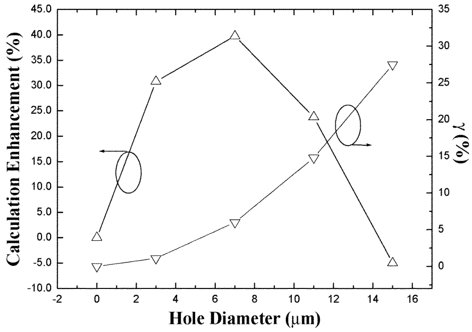

Fig. 5. Showing the calculation enhancement of light output power from the microhole array LEDs (simulation) and the $\gamma$, as functions of $d$.

Ni–Au $= 0.5$, etc. [14]. The emission power densities in the active regions of all devices were set identical in the simulation. Fig. 5 plots the factor by which the light output power of various microhole array LEDs exceeds that of a conventional BA LED and the ratio ($\gamma$) of the etched (lose) light-generating-area of a microhole array LED to the mesa area of a conventional BA LED, as functions of $d$. The enhancement factor of the microhole array LED with $d = 7\ \mu$m is $\sim$39% and is similar to the experimental values, 36%, slightly exceeding it perhaps because nonradiative recombination on the etched sidewall surfaces of the microhole array LEDs. Additionally, in Fig. 5, the enhancement factor decreases as $\gamma$ increases above 6% ($d > 7\mu$m) and no enhancement is observed from the microhole array LEDs at $\gamma > 28\%$. The large increase in the surface areas efficiently promotes the extraction of the photons that propagate in-plane and the scattering of light off of the sidewalls in the microholes. A fraction of the light-generating-area of the microhole array LEDs was etched, producing a less active region in the microhole array LEDs than that in the conventional BA LEDs. The competition between the improvement in light extraction and the reduction in the area of the active region importantly affects the light output. Accordingly, optimally designing microhole array LEDs considerably improves the light output efficiency.

## IV. CONCLUSION

Highly efficient InGaN-based microhole array LEDs were fabricated. Their characteristics were measured and compared with those of conventional BA LEDs fabricated from the same wafer. The light output from the microhole array LEDs was over 36% grater than that from conventional LEDs with the same device areas. In particular, microhole array LEDs exhibited not enhancement when $\gamma > 28\%$. These facts are attributable to combination of the enhancement in extraction efficiency by increasing the area of the sidewall surfaces and the reduction of the active areas of the microhole array LEDs. Optimally designed InGaN-based microhole array LEDs exhibit improved light output efficiently and are candidates for white-light LEDs or high-power/high-efficiency large-area LEDs.

## ACKNOWLEDGMENT

The authors would like to thank Prof. S. T. Yen and Y. C. Chen of the Department of Electronics Engineering, National Chiao Tung Uiversity, Taiwan, R.O.C., for their valuable discussions and technical support.

## REFERENCES

[1] O. Ambacher, W. Rieger, P. Ansmann, H. Angerer, T. D. Moustakas, and M. Stutzmann, “Sub-bandgap absorption of gallium nitride determined by photothermal deflection spectroscopy,” *Solid State Commun.*, vol. 97, pp. 365–357, 1996.

[2] M. y. Broditsk and E. Yablonovitch, “Light-emitting diode extraction efficiency,” in *Proc. SPIE*, vol. 3002, 1997, pp. 119–122.

[3] S. X. Jin, J. Li, J. Y. Lin, and H. X. Jiang, “InGaN/GaN quantum well interconnected microdisk light emitting diodes,” *Appl. Phys. Lett.*, vol. 77, pp. 3236–3238, 2000.

[4] H. W. Choi, C. W. Jeon, and M. D. Dawson, “InGaN microring light-emitting diodes,” *IEEE Photon. Technol. Lett.*, vol. 16, no. 1, pp. 33–35, Jan. 2004.

[5] H. W. Choi, C. W. Jeon, M. D. Dawson, P. R. Edward, R. W. Martin, and S. Tripathy, “Mechanism of enhanced light output efficiency in InGaN-based microlight emitting diodes,” *J. Appl. Phys.*, vol. 93, pp. 5978–5980, 2003.

[6] R. A. Mair, K. C. Zeng, J. Y. Lin, H. X. Jiang, B. Zhang, L. Dai, H. Tang, A. Botchkarev, W. Kim, and H. Morkoc, “Optical properties of GaN/AlGaN multiple quantum well microdisks,” *Appl. Phys. Lett.*, vol. 71, pp. 2898–2900, 1997.

[7] K. C. Zeng, L. Dai, J. Y. Lin, and H. X. Jiang, “Optical resonance modes in InGaN/GaN multiple-quantum-well microring cavities,” *Appl. Phys. Lett.*, vol. 75, pp. 2563–2565, 1999.

[8] J. K. Sheu, G. C. Chi, and M. J. Jou, “Low-operation voltage of InGaN/GaN light-emitting diodes by using a Mg-doped Al0.15Ga0.85N/GaN superlattice,” *IEEE Electron Device Lett.*, vol. 22, no. 4, pp. 160–162, Apr. 2001.

[9] S. J. Chang, C. S. Chang, Y. K. Su, R. W. Chuang, W. C. Lai, C. H. Kuo, Y. P. Hsu, Y. C. Lin, S. C. Shei, H. M. Lo, J. C. Ke, and J. K. Sheu, “Nitride-based LEDs with an SPS tunneling contact layer and an ITO transparent contact,” *IEEE Photon. Technol. Lett.*, vol. 16, no. 4, pp. 1002–1004, Apr. 2004.

[10] J. K. Sheu, Y. K. Su, G. C. Chi, P. L. Koh, M. J. Jou, C. M. Chang, C. C. Liu, and W. C. Hung, “High-transparency Ni/Au ohmic contact to p-type GaN,” *Appl. Phys. Lett.*, vol. 74, pp. 2340–2342, 1999.

[11] N. Blanc, P. Gueret, P. Buchmann, K. Datwyler, and P. Vettiger, “Conductance statistics of small-area ohmic contacts on GaAs,” *Appl. Phys. Lett.*, vol. 56, pp. 2216–2219, 1990.

[12] E. D. Haberer, M. Woods, A. Stonas, C. –H. Chen, S. Keller, M. Hansen, U. Mishra, S. DenBaars, J. Bowers, and E. L. Hu, “Investigation of sidewall recombination in GaN using a quantum well probe,” in *Mater. Res. Soc. Symp. Proc.*, vol. 639, 2000, Paper G11.21.

[13] D. Eisert and V. Harle, “Simulations in the development process of GaN-based LED’s and laser diodes,” in *Int. Conf. Numerical Simulation of Semiconductor Optoelectronic Devices*, 2002, Session 3: Photonics Devices, invited paper.

[14] C.-C. Kao, H. C. Kuo, H. W. Huang, J. T. Chu, Y. C. Peng, Y. L. Hsieh, C. Y. Luo, S. C. Wang, C. C. Yu, and C. F. Lin, “Light-output enhancement in a nitride based light-emitting diode with 22° undercut side walls,” *IEEE Photon. Technol. Lett.*, vol. 17, no. 1, pp. 19–21, Jan. 2005.